Prognostic significance of abnormal matrix collagen remodeling in colorectal cancer based on histologic and bioinformatics analysis

YUQI LIANG[1,2], ZHIHAO LV[3], GUOHANG HUANG[4], JINGCHUN QIN[1,2],
HUIXUAN LI[1,2], FEIFEI NONG[1,2] and BIN WEN[1,2]

[1]Department of Science and Technology Innovation Center, Guangzhou University of Chinese Medicine; [2]Department of PI-WEI Institute of Guangzhou University of Chinese Medicine, Guangzhou, Guangdong 510000; [3]Department of Anorectal Surgery, Zhongshan Hospital Affiliated to Guangzhou University of Chinese Medicine, Zhongshan, Guangdong 528400; [4]Department of Rehabilitation Sciences, The Hong Kong Polytechnic University, Hong Kong, SAR 999077, P.R. China

Abstract. As the major component of the tumor matrix, collagen greatly influences tumor invasion and prognosis. The present study compared the remodeling of collagen and collagenase in 56 patients with colorectal cancer (CRC) using Sirius red stain and immunohistochemistry, exploring the relationship between collagen remodeling and the prognosis of CRC. Weak or strong changes in collagen fiber arrangement in birefringence were observed. With the exception of a higher density, weak changes equated to a similar arrangement in normal collagen, while strong changes facilitated cross-linking into bundles. Compared with normal tissues, collagen I (COL I) and III (COL III) deposition was significantly increased in CRC tissues, and was positively correlated with the metastasis status. In tissues without distant metastasis, collagen IV (COL IV) levels were higher than that in normal tissues, while in tissues with distant metastasis, collagen IV expression was significantly lower. Furthermore, the expression of matrix metalloproteinase (MMP)-1, MMP-2, MMP-7, MMP-9 and lysyl oxidase-like 2 (LOXL2) was found to be elevated in the cancer stroma, which contributed to the hyperactive remodeling of collagen. The association between collagen-related genes and the occurrence and prognosis of CRC were analyzed using biometric databases. The results indicated that patients with upregulated expression of a combination of coding genes for collagen and collagenase exhibited poorer overall survival times. The coding genes *COL1A1-2*, *COL3A1*, *COL4A3*, *COL4A6* and *MMP2* may therefore be used as biomarkers to predict the prognosis of patients with CRC. Furthermore, the results of Gene Ontology (GO) and Kyoto Encyclopedia of Genes and Genomes (KEGG) analysis suggest that collagen may promote tumor development by activating platelets. Collectively, the abnormal collagen remodeling, including associated protein and coding genes is associated with the tumorigenesis and metastasis, affecting the prognosis of patients with CRC.

Introduction

Colorectal cancer (CRC) has a high global incidence and mortality rate (1). Tumor metastasis is often associated with poor prognosis and is the primary cause of death in patients with cancer (2). Existing research shows that the tumor matrix has profound influences on tumor growth and metastasis (3). As the core constituent of the tumor matrix, collagen provides a mechanical or signaling support for tumor growth and metastasis and is related to prognosis (4,5). Several studies have shown that collagen is the migratory channel of cancer cells, controlling the metastasis of various tumor cells (6-8). Bonnans *et al* (9) revealed that dense deposition of COL I may increase the risk of tumor metastasis and worse prognosis.

Tumor progression is accompanied by an abnormal remodeling of the matrix collagen. Histologically, abnormal remodeling of collagen mainly results in excessive deposition, altered-proportions and changed-arrangement of collagen (10-12). In normal tissues, the collagen fibers of the tumor matrix are curly with an irregular arrangement, while in tumor tissues, especially those with metastasis, the fibers are linearized and dense with a directional arrangement (13). Tanjore and Kalluri (14) identified numerous hidden carcinogen-containing domains within collagen that were exposed following collagen remodeling, and which subsequently facilitated tumor metastasis.

Collagen remodeling is induced by collagenase. The most common collagenases are the matrix metalloproteinase (MMP) and lysine oxidase (LOX) families, which facilitate the degradation or cross-link of collagen, respectively (15,16). In various types of cancers, such as breast cancer and hepatocellular carcinoma, the overproduction of these collagenases has been found to promote abnormal collagen remodeling (17-19). The

---

changes in the deposition and the ratio of subtypes of collagens are also regulated by their associated coding genes. The mRNA level of these coding genes can affect tumor occurrence and prognosis (20,21), but their prognostic significance in CRC is not totally clear.

The tumor invasion front is the area at the edge of the tumor which represents a critical interface at tumor progression and tumor cell dissemination (22). Changes in the environment of the tumor invasion front also affect the behavior of tumor cells and patient prognosis (23). However, there are few studies focused on the association between the matrix collagen at the tumor invasion front and CRC development and prognosis. Based on these perspectives, the changes in collagen arrangement and expression at the tumor invasion front were analyzed in CRC patients with and without metastasis, as well as the corresponding differences in collagenase expression. In addition, bioinformatics analysis from multiple biometric databases was performed to study the expression and prognostic significance of matrix collagen and collagenase genes in CRC.

Materials and methods

Patients and specimens. A total of 56 patients (age, 26-86 years) undergoing colonoscopic polypectomy at the First Affiliated Hospital of Guangzhou University of Chinese Medicine (Guangzhou, China) between July 2018 and January 2020 were enrolled in the present study. Patients who had received neoadjuvant radiotherapy, chemotherapy or chemoradiotherapy were excluded. Clinical and pathological data including pathology reports, sex, age at surgical intervention, macroscopic classification, tumor location, tumor size, tumor differentiation, lymphovascular infiltration and depth of invasion, were collected from medical records. The American Joint Commission on Cancer TNM staging system was used to clinical stage the tumors (24). Tissues from the tumor invasion front were obtained from the edge of each tumor, and normal-adjacent tissues were obtained 5.0-10.0 cm away from the primary tumor. The 112 samples were then divided into metastatic, non-metastatic and normal groups (from metastatic patients) and normal groups (from non-metastatic patients). This study was approved by the Ethics Committee of First Affiliated Hospital of Guangzhou University of Chinese Medicine [No. Y (2019)172] and written informed consent was obtained from all patients. The study was performed in accordance with the Declaration of Helsinki.

Immunohistochemistry (IHC). Tissues were fixed with 4% paraformaldehyde at room temperature for 24 h and serially cut into 4-μm-thick sections for IHC. The primary antibodies are displayed in Table SI. The paraffin-embedded sections were dewaxed, rehydrated in a descending alcohol series, and heated in citrate buffer (pH 6.0) for 20 min at 95℃. The sections were quenched to block endogenous peroxidase activity (3% endogenous peroxidase blocker at room temperature for 10 min), and then blocked with normal goat serum for 20 min at 37℃. The sections were incubated with primary antibodies for 16 h at 4℃, rinsed with wash buffer, and then incubated with secondary antibodies at 37℃ for 15 min, horseradish peroxidase-labeled streptomycin was subsequently added, and the slides were

visualized using a 3,3-diaminobenzidine tetrahydrochloride substrate kit (DAB; ZLI-9018; ZSGB-BIO; OriGene Technologies, Inc.). The sections were lightly counterstained with hematoxylin, dehydrated, cleared and mounted with resin. Negative controls were prepared by omitting the primary antibodies, while keeping all other procedures the same.

For immunohistochemical quantification, images of three randomly selected microscopic fields per slide were captured using a an Olympus BX 51 fluorescence microscope (Olympus Corporation; magnification, x200); and evaluated by independent pathologists. Image Pro Plus 6.0 (Media Cybernetics, Inc.) was used for digital image analysis. The scores for staining intensity and the percentage of positive cells were multiplied; the yellow density reflects the expression level of the target protein. The expression levels of COL I, III, and IV, MMP-1, MMP-2, MMP-7, and MMP-9, as well as LOXL2 were quantified via the average optical density (AOD).

Sirius red staining and quantification. The tissue sections were deparaffinized and rehydrated in a graded ethanol series, and then incubated for 1 h in Sirius red stain (G1018; Servicebio). The stained sections were analyzed using an Olympus IX73 inverted microscope (Olympus Corporation; magnification, x200 or x400) with a linear polarizer. To avoid missing any details, the filter was tilted to an angle between 0 and 90 until the birefringence became evident and the background became completely black; the focus was then corrected once more (25). The halogen lamp intensity and exposure time were constant within each image. Under polarized light, COL I appears red or yellow with strong birefringence, while COL III is green with weak birefringence. The areas of COL I and III staining were analyzed using Image Pro Plus 6.0 (Media Cybernetics, Inc.).

Protein functional annotation. The Search Tool for Recurring Instances of Neighbouring Genes (STRING) database (https://string-db.org) is designed to evaluate the integration of protein-protein interactions, including direct (physical) and indirect (functional) associations (26). The STRING database was used to detect the potential associations among MMP-1, MMP-2, MMP-7 and MMP-9 and LOXL2.

Differential mRNA expression between tumor and normal tissues. The Oncomine database (https://www.oncomine.org/) was used to analyze the mRNA expression levels of coding genes (*COL1A1-2, COL3A1, COL4A1-6, LOXL2*, and *MMP1, MMP2, MMP7* and *MMP9*) in different types of cancer. The search was conducted using the following criteria: i) type of analysis: Cancer vs. normal tissues; ii) type of data: mRNA; iii) thresholds: Fold change=2 and P=0.01. Then UCSC Xena Browser (27) (https://xenabrowser.net/datapages/) was then used to obtain the TCGA-COADREAD gene expression dataset and corresponding clinical data, which includes 383 tumor samples and 51 normal samples. The data were used to verify the differential mRNA expression levels of the target genes in CRC and control normal tissues. P<0.01 was considered to indicate a statistically significant difference.

Functional and pathway enrichment analysis. The Database for Annotation, Visualization and Integrated Discovery (DAVID) (https://david.ncifcrf.gov) integrates biological data

and analysis tools to generate systematic and comprehensive functional annotations (28). In the presents study, DAVID was used to conduct Gene Ontology (GO) and the Kyoto Encyclopedia of Genes and Genomes (KEGG) analysis of related coding genes. GO analyses classified the coding genes into three categories, biological process (BP), cellular component (CC) and molecular function (MF). KEGG analyses were conducted to identify the pathways in which the coding genes were significantly enriched; $P<0.05$ and an enrichment score (ES) >1.0 were used as the cutoff criteria for significance.

Cox proportional hazards regression analysis. The gene expression profiles and corresponding clinical data of the GSE17536 dataset (29) were downloaded using the Gene Expression overview database (GEO, https://www.ncbi.nlm. nih.gov/geo/). Samples without overall survival (OS) events (time from surgery to death) and OS times were removed, and the remaining 177 CRC samples were included in the present study. Next, univariate and multivariate Cox proportional risk regression analyses were used to analyze the coding genes. Based on the expression and coefficients of these coding genes, the 'coxph' function in the R 'survival' package (http://cran.r-project.org/package=survival) (30) was used to calculate the risk score for each patient and to establish an optimal prognostic model.

Survival analysis. Survival analysis for the coding genes in CRC (*COL1A1-2*, *COL3A1*, *COL4A1-6*, *LOXL2*, and *MMP1*, *MMP2*, *MMP7* and *MMP9*) was performed using the PROGgeneV2 prognostic database (http://genomics. jefferson.edu/proggene/index.php) (31). Briefly, the following parameters were selected in the first interface: '*COL1A1, COL1A2, COL3A1, COL4A1, COL4A2, COL4A3, COL4A4, COL4A5, COL4A6, MMP1, MMP2, MMP7, MMP9* and *LOXL2*' in multiple user input genes; 'combined signature graphs only'; 'colorectal cancer' in cancer type; 'death' in survival measure; and 'median' in bifurcate gene expression. Then, in the second interface, filter 'GSE17536' was selected, and the plot was created. The log-rank P-value and hazard ratio (HR) with 95% confidence interval were calculated and displayed on the webpage. Only data with $P<0.05$ were selected for analysis.

Data from the GSE39582 dataset (32) in the Gene Expression overview database (GEO, https://www.ncbi.nlm.nih.gov/geo/) were used to externally validate the survival effects of six genes in the prognostic model. Analysis was performed using the R 'survminer' package (https://CRAN.R-project. org/package=survminer).

Statistical analysis. Statistical differences between COL I, COL III and COL IV, and COL I/COL III, COL I area/COL III area, MMP-1, MMP-2, MMP-7, MMP-9 and LOXL2 between metastasis and non-metastasis were evaluated by unpaired t-tests; while between metastasis and normal sample (metastasis), or non-metastasis and normal sample (non-metastasis), paired t-tests were utilized. In addition, COL IV (Fig. 2I) was further separated into six groups: Distant-metastasis, lymphatic-metastasis, non-metastasis and normal sample (distant-metastasis), normal sample (lymphatic-metastasis),

normal sample (non-metastasis). The comparison among distant-metastasis, lymphatic-metastasis, non-metastasis was evaluated by Welch's ANOVA, and Dunnett's T3 test was used to post hoc comparison; while the comparison between distant-metastasis and normal sample (distant-metastasis), lymphatic-metastasis and normal sample (lymphatic-metastasis) or non-metastasis and normal sample (non-metastasis) was analyzed by paired t-tests. P-values from Welch's ANOVA were adjusted for multiple comparisons using Bonferroni corrections. Pearson's correlation analysis was conducted to determine the associations between the following: The expression of MMP-7 and MMP-1, MMP-2 or MMP-9; and the expression of LOXL2 and MMP-1, MMP-2, MMP-7 or MMP-9. The associations between the clinical parameters and immunohistochemical results were analyzed using with the Chi-squared test or Fisher's exact test (one or more cell contains a count of 5 or fewer; such as the age of MMP-2, MMP-7, MMP-9 and LOXL2; the differentiation of all index; the clinical stage of COL I, COL I area, COL III area, COL I/COL III, COL I area/COL III area, MMP-1, MMP-9 and LOXL2; the T-stage of COL III; the condition of metastasis of all index). Statistical analyses were conducted using SPSS version 25.0 for Windows (IBM, Corp.), and $P<0.05$ was considered to indicate a statistically significant difference.

Differentially expressed coding genes between CRC and normal tissue samples were assessed using the R 'limma' package (version 3.32.10) (33). Volcano plots were constructed using the volcano plotting tool (https://shengxin. ren), and the Bioinformatics and Evolutionary Genomes website (http://bioinformatics.psb.ugent.be/webtools/Venn/) was used to create the Venn diagram. OS was analyzed by Kaplan-Meier survival curve analysis and significance was determined using the log-rank test. Time-dependent receiver operating curve (ROC) analysis was performed to assess the sensitivity and specificity of the signature prognosis prediction. Statistical analysis was performed: $^{**}P<0.01$; $^{*}P<0.05$; $^{ns}P>0.05$ (as indicated in the images with the relevant symbols).

Results

Alterations in collagen arrangement at the CRC tumor invasion front. As one of its essential characteristics, collagen arrangement is subsequently influenced by collagen remodeling. In the present study, the collagen fibers in the normal intestinal mucosa were thin, wavy and dispersed (Fig. 1A). However, at the CRC tumor invasion front, the collagens fibers were arranged differently; the fibers with weak changes were more linearized and denser than normal collagen fibers (Fig. 1A). The collagen fibers with strong changes exhibited an evident increase in density and were crosslinked into bundles with a more uniform arrangement (Fig. 1A). Furthermore, among the 27 metastatic CRC samples, 23 exhibited strong changes in collagen fibers, while only 4 samples exhibited weak changes (Fig. 1B). Of the 29 non-metastatic samples, 20 exhibited weak changes, and 9 possessed strong changes (Fig. 1B). These results indicate that collagen arrangement affects the development of CRC.

Expression of COL I, III and IV in CRC. Collagen expression patterns are another essential aspect of collagen characteristics.
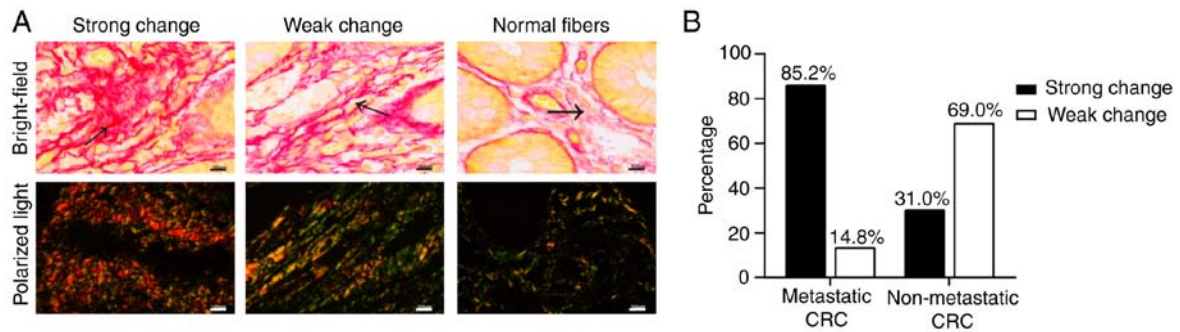
Figure 1. Changes in collagen fiber arrangement differ in different cases of CRC. Differences are indicted by black arrow. (A) Representative images of collagen fiber arrangement characteristics. (B) Comparison of the remodeling intensity of collagen arrangement in metastatic and non-metastatic CRC. Magnification, x400; Scale bar, 100 μm. CRC, colorectal cancer.
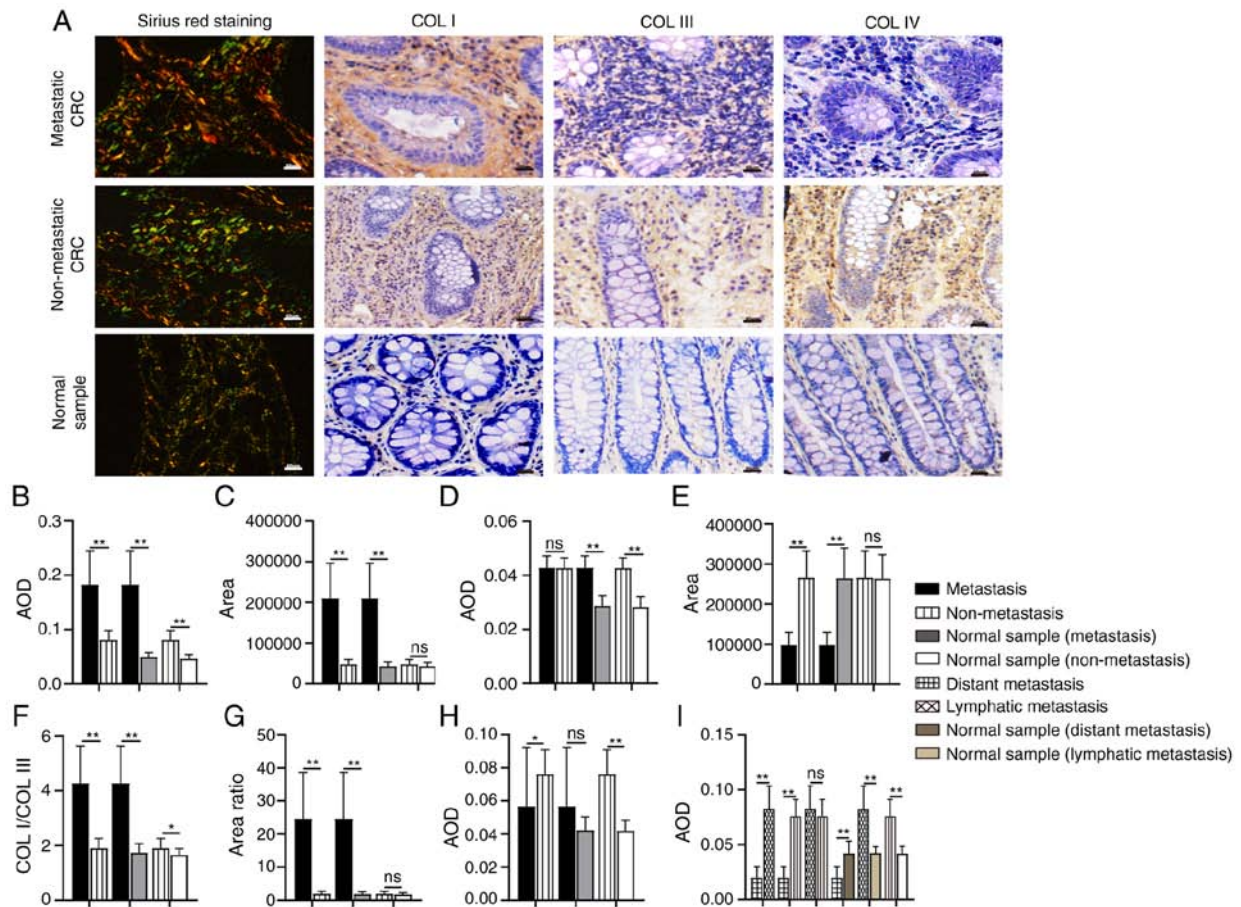

Figure 2. Comparison of collagen expression in different tissue samples. (A) Images and expression levels of COL I, COL III, and COL IV in different tissue samples. (B-I) Differences in the expression of (B) COL I, (C) COL I area, (D) COL III, (E) COL III area, (F) the ratio of COL I/COL III, (G) the ratio of COL I area/COL III area, and (H and I) COL IV. Magnification, x200. Scale bar, 50 μm. COL, collagen; AOD, average optical density; CRC, colorectal cancer. *P<0.05; **P<0.01; nsP>0.05.

During tumor development, the expression level, distribution and the ratio of collagens are altered. COL I, III and IV are the most common matrix collagens. In the present study, the expression level and distribution of COL I, III, and IV was detected by IHC and Sirius red staining, respectively (Fig. 2A). COL I is the most abundant collagen type in the tumor matrix and is mainly distributed in the interstitial matrix (IM), while COL III is mostly distributed along with COL I. In addition, a changed COL I/III ratio influences the hardness of the tumor matrix, regulating tumor growth and migration (10,11). The results of IHC showed that the expression of COL I in metastatic CRC was significantly higher than that in non-metastatic CRC (P<0.01; Fig. 2B) and normal tissues (P<0.01; Fig. 2B); COL I expression in non-metastatic CRC was also higher than that in the normal samples (P<0.01). There was no significant difference in the expression of COL III between metastatic and non-metastatic CRC samples (P=0.928; Fig. 2D), although its expression in metastatic and non-metastatic CRC was higher than that in corresponding normal tissues, respectively (P<0.01). Moreover, the COL I/COL III ratio was significantly
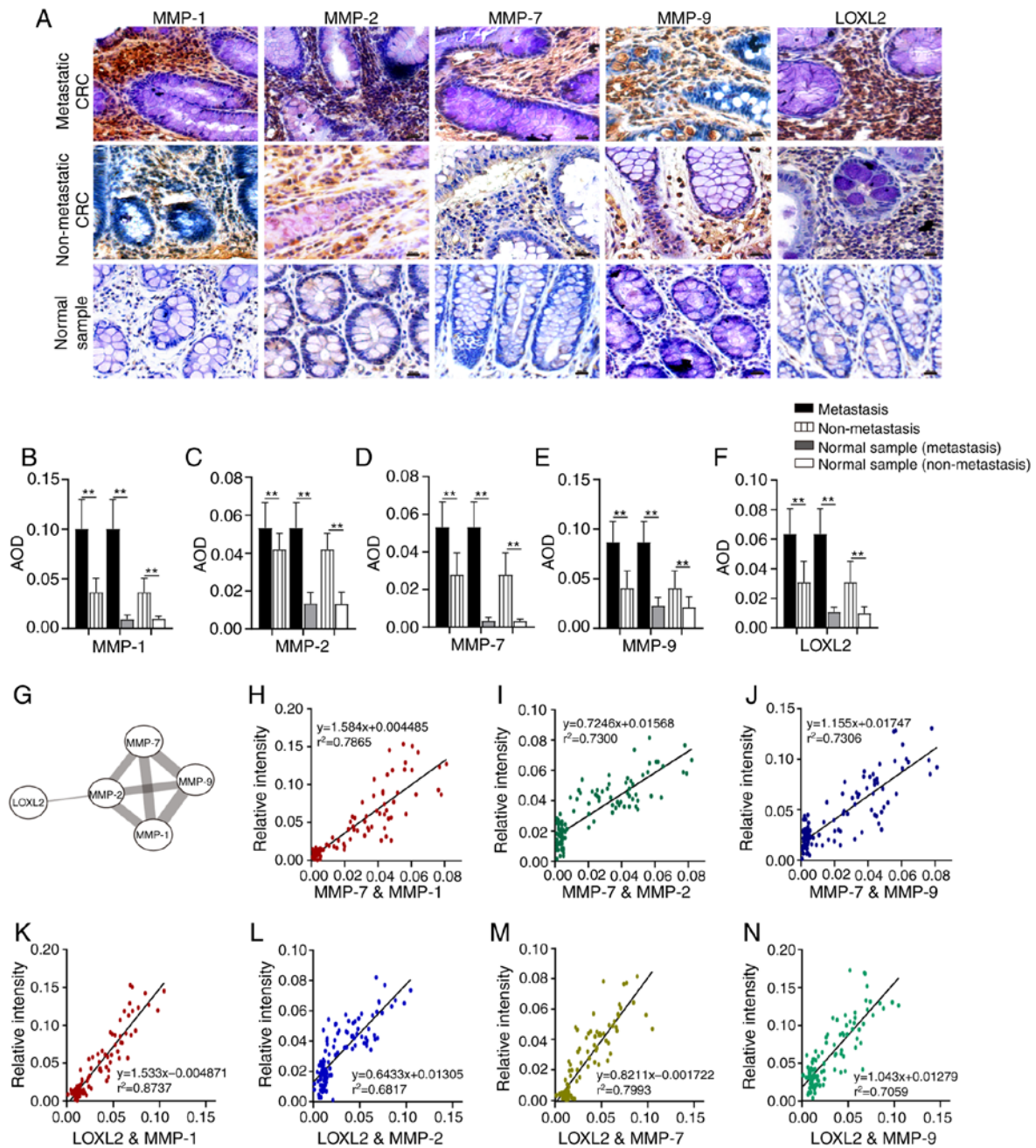
Figure 3. Comparison of collagenase expression levels in different tissue samples. (A) Images of MMP-1, MMP-2, MMP-7, MMP-9 and LOXL2 in different tissue samples. (B-F) The expression levels of (B) MMP-1, (C) MMP-2, (D) MMP-7, (E) MMP-9 and (F) LOXL2 in different tissue samples. (G) Interactions between LOXL2 and MMP-1, MMP-2, MMP-7 and MMP-9. (H-J) Correlation analysis between the expression of (H) MMP-7 and MMP-1, (I) MMP-7 and MMP-2 and (J) MMP-7 and MMP-9. (K-N) Correlation analysis between the expression of (K) LOXL2 and MMP-1, (L) LOXL2 and MMP-2, (M) LOXL2 and MMP-7 and (N) LOXL2 and MMP-9. Magnification, x200; Scale bar, 50 μm. MMP, matrix metalloproteinase; LOXL2, lysyl oxidase-like 2; AOD, average optical density; CRC, colorectal cancer. **$P<0.01$.

increased in the metastatic CRC group (P<0.01; Fig. 2F), although there were significant differences in expression between the non-metastatic CRC and corresponding normal tissue samples (P<0.05).

Sirius red staining reveals thick, strongly birefringent COL I fibers (red), while COL III appears as thin, weakly birefringent green fibers (34). In the present study, collagens in metastatic CRC were mostly reddish or yellowish-orange, while collagens in the normal samples were a yellowish-green color. In non-metastatic CRC, the proportions of the two colors were similar (Fig. 2A). Moreover, compared with

non-metastasis CRC, in metastatic CRC, the area of COL I was significantly expanded (P<0.01; Fig. 2C), the area of COL III was significantly decreased (P<0.01; Fig. 2E), and the ratio of COL I area/COL III area was significantly increased (P<0.01; Fig. 2G). In the non-metastatic CRC and corresponding normal samples, there was no significant difference in COL I area (P=0.051; Fig. 2C) and COL III area (P=0.901; Fig. 2E), or in the ratio between the two (P=0.197; Fig. 2G).

COL IV is mainly distributed in the basal membrane (BM). The remodeling of COL IV would destroy the continuity and integrity of the BM and contribute to tumor metastasis (35).

Table I. Clinicopathological characteristics of the CRC patients (N=56).

Characteristics	n	%
Sex		
Male	31	55.4
Female	25	44.6
Age (years)		
<50 (mean age, 45)	11	19.6
≥50 (mean age, 63)	45	71.4
Condition of metastasis		
Metastasis	27	48.2
Non-metastasis	29	51.8
Differentiation		
Well differentiation	2	3.6
Moderate	46	82.1
Poor	8	14.3
Clinical stage		
I	12	21.4
II	17	30.4
III	16	28.6
IV	11	19.6
T-stage		
T1	5	8.9
T2	12	21.4
T3	38	67.8
T4	1	1.9

CRC, colorectal cancer.

The expression of COL IV in non-metastatic CRC was significantly higher than that in metastatic CRC (P<0.05; Fig. 2H) and corresponding normal tissue samples (P<0.01, Fig. 2H), while the difference between the metastatic CRC and corresponding normal samples was not statistically significant (P=0.053). To verify the significance of COL IV in distant metastasis, the metastatic CRC group was divided into 'distant metastasis' and 'lymph node metastasis only' according to the degree of metastasis. The expression of COL IV in subjects with distant metastases was significantly decreased (P<0.01; Fig. 2I), while the expression of COL IV in those with lymph node metastasis only was marginally (but not significantly) higher than that in the non-metastatic group (P=0.282).

High expression levels of MMP-1, MMP-2, MMP-7, MMP-9 and LOXL2 in metastatic CRC. MMPs and LOX family are the members of collagenases which are responsible for the collagen remodeling. MMP-1 is an interstitial collagenase which degrades COL I and III (15), while MMP-2 and MMP-9 largely degrade COL IV (36). As a stromelysin, MMP-7 not only degrades COL IV, promoting tumor invasion, but also regulates the activities of MMP-1, MMP-2 and MMP-9 (37-39). Lysyl oxidase-like 2 (LOXL2) is a member of the LOX family, which influences COL I, III and IV cross-linking and expression (40,41). IHC was used to detect the expression of different collagenases in metastatic CRC, non-metastatic CRC and non-tumor tissues (Fig. 3A). The results illustrate that the expression level of MMP-1, MMP-2, MMP-7, MMP-9 and LOXL2 in metastatic CRC was higher than that in non-metastatic CRC and corresponding normal tissues (P<0.01; Fig. 3B-F). Furthermore, the expression of these proteins in non-metastatic CRC was also higher than that in corresponding normal tissues (P<0.01; Fig. 3B-F). The results of STRING database analysis revealed that there were interactions between MMP-1, MMP-2, MMP-7, and MMP 9, or LOXL2 and MMP-2 (Fig. 3G). Pearson's correlation analysis was used to evaluate the association between MMP-7 and MMP-1, MMP-2 and MMP-9 expression. A strong correlation was found between MMP-7 and MMP-1 (r=0.887; P<0.01; Fig. 3H). There was also a positive correlation between MMP-7 and MMP-2 (r=0.855; P<0.01; Fig. 3I), and MMP-7 and MMP-9 (r=0.855; P<0.01; Fig. 3J). According to the correlation analysis between LOXL2 and MMP-1, MMP-2, MMP-7 and MMP-9, the expression changes in these collagenases were consistent (Fig. 3K-N), and a strong association was identified between LOXL2 and MMP-1 (r=0.935; P<0.01; Fig. 3K). There were also positive correlations between LOXL2 and MMP-7 expression (r=0.894; P<0.01; Fig. 3M), LOXL2 and MMP-9 expression (r=0.840; P<0.01; Fig. 3N) and LOXL2 and MMP-2 (r=0.826; P<0.01; Fig. 3L).

Association between the expression of collagens and associated collagenases and the clinicopathological characteristics of CRC. Patient clinicopathological characteristics are summarized in Table I. The cutoffs for low and high expression were set according to the median value. As shown in Table IIA and B, the expression and area of COL I and COL III, the ratio of COL I/COL III and COL I area/COL III area, and the expression of COL IV, MMP-1, MMP-2, MMP-7, MMP-9 and LOXL2 in 56 specimens were not significantly correlated with patient sex, age or tumor differentiation. The expression of COL I, COL I area, the ratio of COL I/COL III, the ratio of COL I area/COL III area, MMP-1, MMP-7, MMP-9, and LOXL2 was increased in the middle and late stages of CRC (P<0.01), while COL III area was decreased (P<0.01). Moreover, high expression of COL III and MMP-7 was associated with increased infiltration depth (P<0.05). The expression of COL I, COL I area, COL III area, the ratio of COL I/COL III, the ratio of COL I area/COL III area, COL IV, MMP-1, MMP-2, MMP-7, MMP-9, and LOXL2 differed between cases with distant metastasis, lymph node metastasis and non-metastasis, indicating that their expression is associated with tumor metastasis (P<0.05).

Differential expression of collagen-related coding genes in tumor and normal tissues. In order to verify whether the expression changes in COL I, III and IV, and related collagenases influence the occurrence and development of tumors at the mRNA level, the Oncomine database (https://www.oncomine.org) was used to analyze the mRNA levels of related coding genes in different types of tumor and normal tissues. COL I has two coding genes (*COL1A1* and *COL1A2*), and the gene for COL III is *COL3A1*. *COL4A1-A6* are all coding genes for COL IV. The coding genes for MMP-1, MMP-2, MMP-7, MMP-9 and LOXL2 are *MMP1*, *MMP2*, *MMP7*, *MMP9* and *LOXL2*, respectively. As shown in Fig. 4A, the database

Table II. Relationship between the expression of collagens or correlated enzymes and clinicopathological parameters in 56 patients with colorectal cancer.

A, Collagens and clinicopathological parameters

Variable	COLI Expression Low	High	P-value	COLI area Expression Low	High	P-value	COLIII Expression Low	High	P-value	COLIII area Expression Low	High	P-value	COLIV Expression Low	High	P-value	COLI/COLIII Expression Low	High	P-value	COLI area/COLIII area Expression Low	High	P-value
Sex
Male	18	13	0.179	17	14	0.42	17	14	0.42	14	17	0.42	16	15	0.788	18	13	0.179	17	14	0.42
Female	10	15		11	14		11	14		14	11		12	13		10	15		11	14	
Age (years)
≥50	6	5	0.737	6	5	0.737	6	5	0.737	5	6	0.737	6	5	0.737	6	5	0.737	6	5	0.737
<50	22	23		22	23		22	23		23	22		22	23		22	23		22	23	
Differentiation
Poor	25	23	0.705	25	23	0.705	23	25	0.705	23	25	0.705	23	25	0.705	25	23	0.705	25	23	0.705
Advanced/Medium	3	5		3	5		5	3		5	3		5	3		3	5		3	5	
Clinical stage
III+IV	27	2	<0.001[b]	28	1	<0.001[b]	15	14	0.789	1	28	<0.001[b]	11	18	0.061	27	2	<0.001[b]	28	1	<0.001[b]
I+II	1	26		0	27		13	14		27	0		17	10		1	26		0	27	
T-stage
T3+T4	10	7	0.383	10	7	0.383	14	3	0.003[b]	7	10	0.383	8	9	0.771	10	7	0.383	10	7	0.383
T1+T2	18	21		18	21		14	25		21	18		20	19		18	21		18	21	
Condition of metastasis
Lymphatic metastasis	0	11	<0.001[b]	0	11	<0.001[b]	3	8	0.216	11	0	<0.001[b]	11	0	<0.001[b]	0	11	<0.001[b]	0	11	<0.001[b]
Non-metastasis	1	15		0	16		10	6		16	0		6	10		1	15		0	16	
Distant metastasis	27	2		28	1		15	14		1	28		11	18		27	2		28	1	

Table II. Continued.

B, Correlated enzymes and clinicopathological parameters

Variable	MMP-1 Expression Low	High	P-value	MMP-2 Expression Low	High	P-value	MMP-7 Expression Low	High	P-value	MMP-9 Expression Low	High	P-value	LOXL2 Expression Low	High	P-value
Sex															
Male	17	14	0.42	14	17	0.42	15	16	0.788	16	15	0.788	17	14	0.42
Female	11	14		14	11		13	12		12	13		11	14	
Age (years)															
<50	7	4	0.503	7	4	0.503	7	4	0.503	4	7	0.503	4	7	0.503
≥50	21	24		21	24		21	24		24	21		24	21	
Differentiation															
Advanced/Medium	25	23	0.705	23	25	0.705	24	24	>0.999	25	23	0.705	25	23	0.705
Poor	3	5		5	3		4	4		3	5		3	5	
Clinical stage															
I+II	27	2	<0.001[b]	18	11	0.061	23	6	<0.001[b]	25	4	<0.001[b]	25	4	<0.001[b]
III+IV	1	26		10	17		5	22		3	24		3	24	
T-stage															
T1+T2	10	7	0.383	9	8	0.771	12	5	0.042[a]	11	6	0.146	10	7	0.383
T3+T4	18	21		19	20		16	23		17	22		18	21	
Condition of metastasis															
Distant metastasis	0	11	<0.001[b]	1	10	0.007[b]	0	11	<0.001[b]	0	11	<0.001[b]	0	11	<0.001[b]
Lymphatic metastasis	1	15		9	7		5	11		3	13		3	13	
Non-metastasis	27	2		18	11		23	6		25	4		25	4	

[a]Correlation was significant at the 0.05 level (two-tailed). [b]Correlation was significant at the 0.01 level (two-tailed).
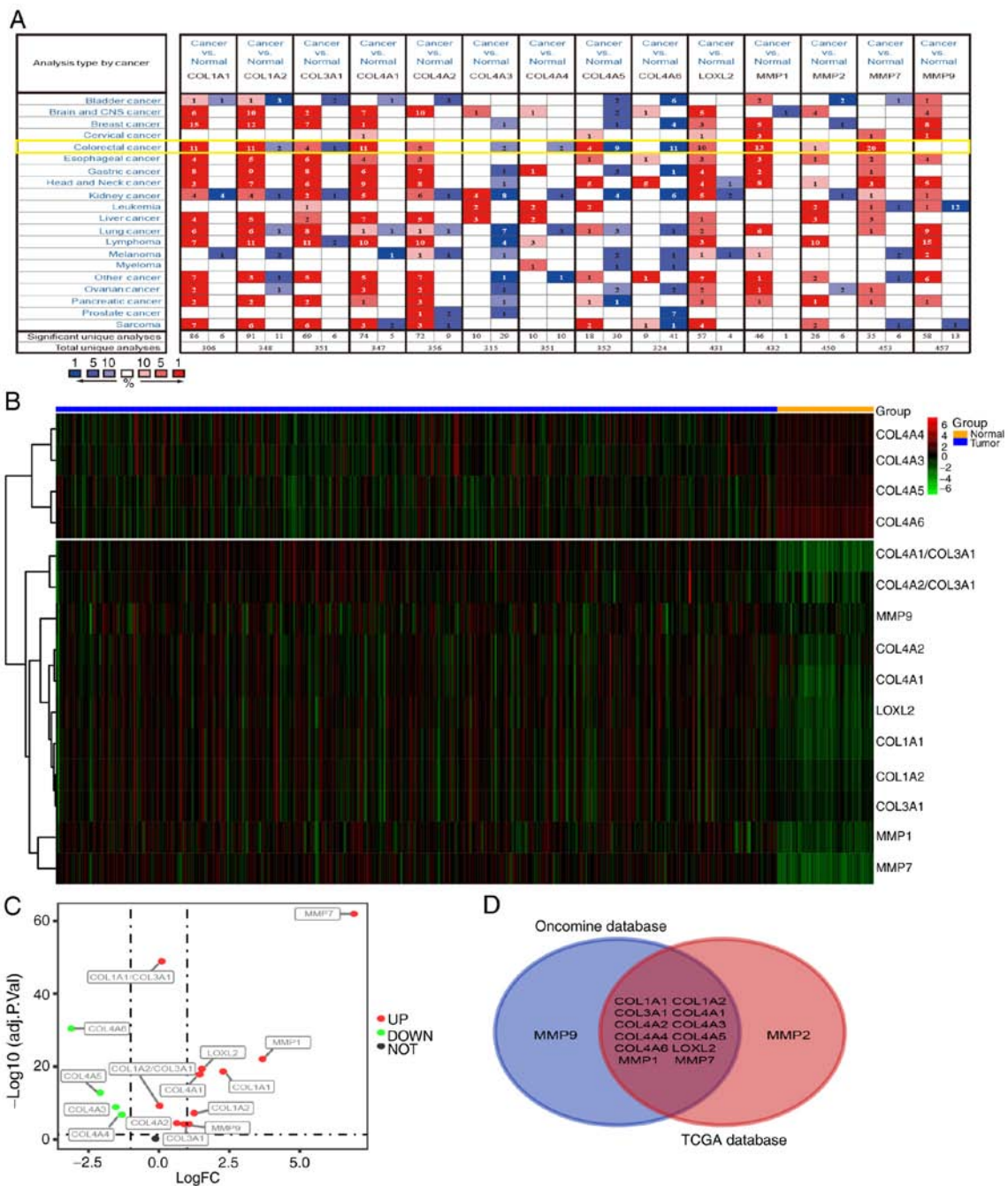
Figure 4. mRNA expression levels of collagens and collagenases in various types of cancer. (A) High or low expression of related coding genes in different types of human cancer tissues, compared with normal tissues, using the Oncomine database (P<0.01). mRNA expression levels in CRC are highlighted in yellow. (B and C) Expression patterns of related coding genes in CRC using TCGA database (P<0.01). (D) Intersection between all related coding genes (n=14) among Oncomine and TCGA expression data. CRC, colorectal cancer; TCGA, The Cancer Genome Atlas.

contains 20 cancer types, (including CRC). *COL1A1*, *COL1A2*, *COL3A1*, *COL4A1*, *COL4A2*, *LOXL2*, *MMP1*, *MMP2*, *MMP7* and *MMP9* were upregulated in the majority of tumor types. On the contrary, the expression of *COL4A3-6* was decreased in tumor tissues. The data from CRC samples revealed that the expression levels of *COL1A1-2*, *COL3A1*, *COL4A1-6*, *LOXL2*, and *MMP1*, *MMP2*, and *MMP7* were different in tumor tissues and normal intestinal tissues, while the expression of *MMP9* was not significantly altered.

Next, CRC RNA-seq data were downloaded from The Cancer Genome Atlas (TCGA) database and subsequently analyzed. The results show that the expression of *MMP7*, *MMP1*, *MMP9*, *LOXL2*, *COL1A1*, *COL1A2*, *COL3A1*, *COL4A1-6*, *COL1A1/COL3A1* and *COL1A2/COL3A1* differed between tumor and normal tissues (logFC>0; P<0.01; Fig. 4B). The levels of *COL4A3*, *COL4A4*, *COL4A5* and *COL4A6* were downregulated in tumor tissues, while the expression of *COL1A1*, *COL1A2*, *COL3A1*, *COL4A1*, *COL4A2*, *LOXL2*, *MMP1*, *MMP7*, *MMP9*, *COL1A1/COL3A1* and *COL1A2/COL3A1* were upregulated (Fig. 4C). The Venn diagram demonstrates the differential expression of *COL1A1-2*, *COL3A1*, *COL4A1-6*, *LOXL2*, *MMP1 and MMP7* in both the Oncomine and TCGA datasets (Fig. 4D), indicating that these genes may have a greater influence on CRC than *MMP2* and *MMP9*.
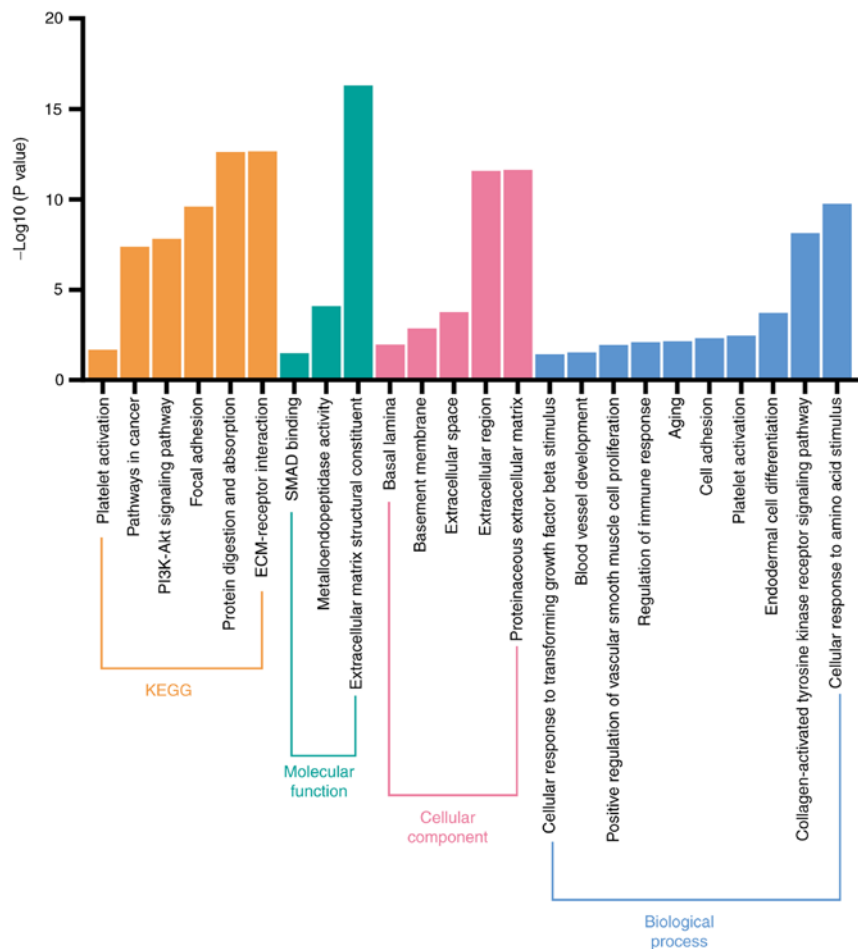
Figure 5. Functional enrichment analysis of coding genes associated with the prognosis of patients with CRC. Functional enrichment analysis including cellular component, molecular function, biological process, and KEGG analysis of 14 coding genes associated with collagen and collagenases. CRC, colorectal cancer; KEGG, Kyoto Encyclopedia of Genes and Genomes.
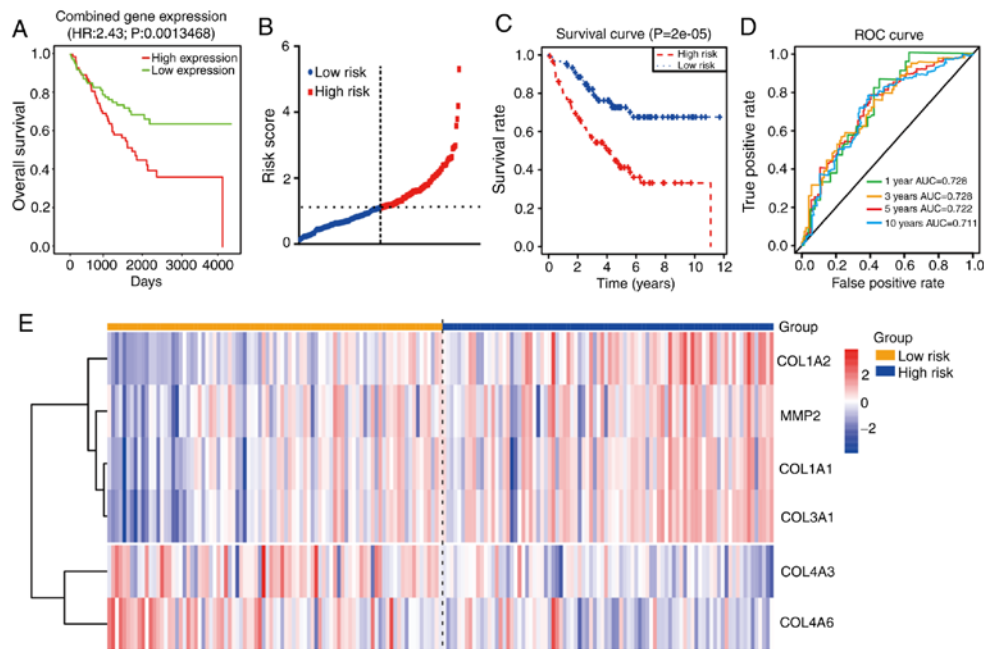

Figure 6. Prognostic analysis of collagen-related coding genes in CRC. (A) OS analysis of combined expression of genes including *COL1A1-2*, *COL3A1*, *COL4A1-6*, *LOXL2*, *MMP1*, *MMP2*, *MMP7* and *MMP9* using PROGgenev2. (B) Time-dependent ROC analysis of the sensitivity and specificity of the six-mRNA signature (*COL1A1-2*, *COL3A1*, *COL4A3*, *COL4A6* and *MMP2*). (C) Kaplan-Meier analysis of the six-mRNA signature. (D) ROC curve of the prognostic model. (E) Heatmap of the expression of the six-mRNA signature. CRC, colorectal cancer; OS, overall survival; ROC, receiver operating characteristic; AUC, area under the curve.

Table III. Univariable Cox regression analysis to assess the prognostic value of each mRNA.

Gene	HR[a]	z	P-value
COL1A2	16.48555	3.440846	0.00058
COL3A1	1954.201	3.115704	0.001835
LOXL2	36.23624	2.900018	0.003731
COL4A5	0.000416	-2.68185	0.007322
COL1A1	48.30721	2.586627	0.009692
COL4A6	2.82E-05	-2.39273	0.016723
COL4A3	0.00033	-2.22433	0.026126
MMP2	12.9414	2.038733	0.041477
COL4A2	21.90964	2.018873	0.0435
COL4A1	23.51048	1.998489	0.045664
COL4A4	3.191615	1.31461	0.188641
MMP1	1.728113	1.10983	0.267072
MMP9	0.398133	-0.91069	0.362457
MMP7	1.382114	0.539802	0.589333

[a]Values >1.0 indicate that expression is positively associated with poor survival. HR, hazard ratio.

Biological pathways involving coding genes associated with collagens and collagenases. The potential biological signaling pathways of 14 collagen-associated coding genes (*COL1A1-2, COL3A1, COL4A1-6, LOXL2, MMP1, MMP2, MMP7* and *MMP9*) were investigated using DAVID. As shown in Fig. 5, KEGG analysis revealed that these coding genes were significantly associated with various pathways, such as those involved in 'platelet activation', 'ECM-receptor interaction', 'PI3K-Akt signaling pathway', and 'focal adhesion'. Furthermore, GO analysis revealed that these genes were significantly enriched in 'platelet activation', 'blood vessel development', and 'collagen-activated tyrosine kinase receptor signaling pathway' to name but a few. Hence, we hypothesized that these genes may affect the progression of patients with CRC primarily via platelet activation and by promoting angiogenesis.

Identification of prognostic genes and establishment of a prognostic model. The PROGgeneV2 database (http://genomics.jefferson.edu/proggene/index.php) was used to determine the impact of collagen and collagenase genes on patient prognosis and survival. Combination analysis of these coding genes suggested that the OS times (Fig. 6A) of the high-expression group were shorter than those in the low-expression group. Moreover, univariate Cox regression analysis of 177 CRC samples from the GSE17536 dataset revealed that seven mRNAs (*COL1A1, COL1A2, COL3A1, COL4A1, COL4A2, LOXL2, MMP2*) were not conducive to the survival of patients with CRC, while the other three mRNAs (*COL4A5, COL4A6 and COL4A3*) were beneficial to survival (P<0.05, Table III). In order to improve the accuracy of the prognostic effect of these mRNA, multivariate Cox analysis was conducted using the 10 candidate mRNAs. Finally, a total of six mRNAs were screened as candidate factors significantly associated with CRC prognosis (P=6.335e-05,

Table IV). Concurrently, a new risk scoring formula was established based on the mRNA expression levels and the coefficients evaluated by multivariate Cox analysis. The mRNA risk score signature=((2.409e+01)*COL3A1) + ((-1.099e+01)*COL4A3) + ((-1.144e+01)*COL4A6) + ((-1.046e+01)*COL1A1) + ((-4.291e+00)*MMP2) + ((2.163e+00)*COL1A2). According to the prognostic model formula, patient risk scores were calculated and ranked, and the risk score distribution is displayed in Fig. 6B. The expression levels of four high-risk mRNAs were higher in the patients with high-risk scores, while the expression levels of two protective mRNAs were higher in the patients with low-risk scores (Fig. 6E).

In order to determine the value of this prognostic model, a total of 177 patients were then separated into high (n=88) and low (n=89) risk score groups. The results showed that the patients in the high-risk group possessed shorter OS times and poorer prognoses than those in the low-risk group (P<0.0001; Fig. 6C). Moreover, time-dependent ROC curve analysis revealed that the prognostic accuracy of this model was 0.728 at 1 or 3 years, 0.722 at 5 years and 0.711 at 10 years (Fig. 6D). These results suggest that this prognostic model (using *COL1A1, COL1A2, COL3A1, COL4A3, COL4A6* and *MMP2* mRNA expression) has high specificity and sensitivity, and may be used effectively predict the prognosis of patients with CRC.

Verification of survival analysis. To further verify the effects of these six signature mRNAs (*COL1A1, COL1A2, COL3A1, COL4A3, COL4A6* and *MMP2*) on the prognosis of patients with CRC, the effects of these genes on OS were assessed using 562 CRC patient samples from the GSE39582 dataset. As shown in Fig. 7, high expression of *COL1A1, COL1A2, COL3A1* and *MMP2* had adverse effects on the OS of patients with CRC, while high expression of COL4A3 and COL4A6 was beneficial to OS. Collectively, the analyses indicate that *COL1A1, COL1A2, COL3A1, COL4A3, COL4A6* and *MMP2* may be used as prognostic biomarkers for CRC.

Discussion

Remodeling of the matrix environment at the tumor invasion front is considered to be a significant predictor of tumor development (23,42). In the present study, tissues were serially cut into 4-μm-thick sections for immunohistochemistry (IHC) and Sirius red staining. By integrating histological and bioinformatics analyses, the characteristics and coding genes of matrix collagen (and related collagenases) at the tumor invasion front were found to be associated with colorectal cancer (CRC) progression and metastasis.

Collagen characteristics in tumors differ greatly from those in healthy tissues, and are characterized by increased deposition and linearization, as well as considerable cross-linking (43). In CRC, tumors with stronger invasion ability exhibited significantly increased collagen density at the tumor invasion front, and collagen fiber arrangement was linearized and bunched with reduced curvature. Moreover, the expression and distribution of COL I was increased significantly in the tumors, compared with normal tissues. Highly cross-linked and linearized collagen fibers act as channels for

Table IV. The coefficient of each gene.

Gene	Coefficient	exp(coef)	se(coef)	z	P-value
COL3A1	2.409e+01	2.908e+10	8.180e+00	2.945	0.00323
COL4A3	-1.099e+01	1.688e-05	4.124e+00	-2.665	0.00771
COL4A6	-1.144e+01	1.072e-05	4.663e+00	-2.454	0.01412
COL1A1	-1.046e+01	2.855e-05	4.450e+00	-2.351	0.01870
MMP2	-4.291e+00	1.369e-02	2.374e+00	-1.808	0.07066
COL1A2	2.163e+00	8.701e+00	1.414e+00	1.530	0.12612

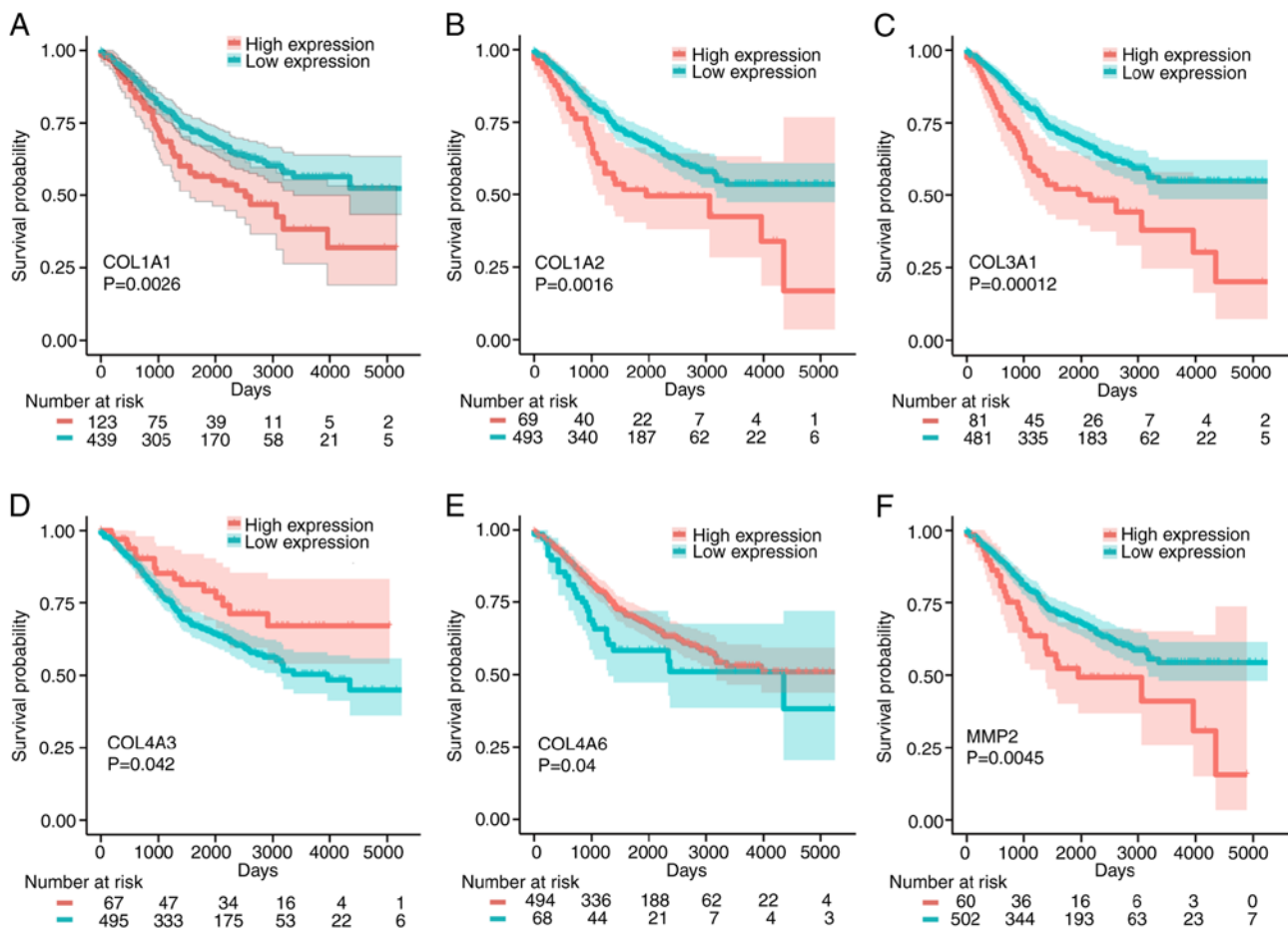Likelihood ratio test=28.91 on 6 genes; P=6.335e-05.

Figure 7. Kaplan-Meier analysis of the association between *COL1A1*, *COL1A2*, *COL3A1*, *COL4A3*, *COL4A6* and *MMP2* and the OS times of patients with CRC. (A) COL1A1, (B) COL1A2, (C) COL3A1, (D) COL4A3, (E) COL4A6 and (F) MMP2. OS, overall survival; CRC, colorectal cancer.

tumor cells, and restriction to these narrow channels, facilitates more precise migration of tumor cells to the preferred destination (44,45). Collagen also promotes tumor invasion and metastasis by expanding the distribution range of tumor cells (46). In addition, changes in the ratio of different matrix collagens also affect tumor progression. The results of the present study demonstrate that the ratio of COL I/COL III increased significantly in the metastatic group. Current studies have also shown that an increased COL I/COL III ratio promotes the migration and distribution of tumor cells by increasing the stiffness of the matrix (10,34). It is also worth noting that the expression of COL III in the matrix also affects the density and arrangement of COL I (47). When studying the properties of matrix collagen in tumors, the effects of more than one type of collagen should be considered.

In addition, changes in matrix collagen fluctuate during the progression of CRC. Fan *et al* (48) indicated that a decrease in COL IV facilitates the invasion of tumor cells, while Öhlund *et al* (49) showed that the excessive accumulation of COL IV was one of the necessary conditions for cancer cell survival. In the present study, the expression of COL IV at the CRC tumor invasion front was significantly decreased

in patients with distant metastasis. The expression of COL IV in patients with lymph node metastasis was not significantly different from that in patients without metastasis, and expression was higher than that in distal normal tissues. Based on the aforementioned findings, we hypothesize that unlike the consistent increase in COL I and COL III expression, both the upregulation and absence of COL IV expression can promote CRC development, which is detrimental to patient prognosis. Therefore, in patients with CRC, changes in the remodeling and expression of different collagens should be comprehensively analyzed at different stages of tumor progression.

Matrix collagen remodeling is largely regulated by the LOX and MMP family (50). The present study revealed that the expression of LOXL2, MMP-1, MMP-2, MMP-7 and MMP-9 at the tumor invasion front was significantly higher in the metastatic group than in the non-metastatic and normal groups. Previous studies have also shown that these proteins may enhance tumor cell invasiveness by remodeling the tumor microenvironment, and may also be associated with poor prognosis (51,52). Although the cross-linking effect of LOXL2 opposes the degradation abilities of MMP-1, MMP-2, MMP-7 and MMP-9, the expression of one does not restrict the abilities of the other. Liu *et al* (53) also found that LOXL2 regulates the activity of MMPs, and when LOXL2 was highly expressed, MMP-9 activity was also increased. In the current study, correlation analysis of LOXL2, MMP-1, MMP-2, MMP-7 and MMP-9 indicated that LOXL2 expression was positively correlated with that of MMP-1, MMP-2, MMP-7 and MMP-9. STRING database analysis also revealed an interaction between LOXL2 and MMP-2. Although the mechanism of LOXL2 and MMPs remains unclear, these data show that LOXL2 and the MMPs jointly regulate collagen remodeling. Collagen remodeling is more active during metastasis (4), and the activities of LOXL2, MMP-1, MMP-2, and MMP-9 are also significantly increased.

The synthesis of matrix collagen and associated collagenases is regulated by their coding genes. The results of the present study indicate that abnormal changes in the expression of these genes (*COL1A1-A2, COL3A1, COL4A1-A6, MMP1, MMP2, MMP7, MMP9* and *LOXL2*) are involved in CRC development, and also affect the prognosis of patients with CRC. This result further verified that abnormal expression of collagen and related collagens is related to the occurrence and prognosis of CRC. The effects of these coding genes on CRC prognosis were comprehensively analyzed, and a prognostic model of CRC was constructed with six mRNA signatures (*COL1A1, COL1A2, COL3A1, COL4A3, COL4A6* and *MMP2*). Among them, *COL1A1, COL1A2, COL3A1* and *MMP2* have been reported to serve vital roles in tumor invasion, and are thus associated with poor prognosis (54-57). *COL4A3* and *COL4A6*, encoding COL IV alpha chains 3 and 6, respectively, are required for correct basement membrane (BM) formation, and mutations within these genes affect BM stability (58,59). Moreover, GO and KEGG analyses showed that these coding genes are primarily associated with platelet activation pathways. It has also been reported that the collagen or collagenases on the surface of tumor cells binds to integrins on the surface of platelets, inducing platelet activation (60,61). Following activation, platelets induces tumor angiogenesis by releasing

associated growth factors, which subsequently promotes tumor growth (62). The binding of platelets to cancer cells protects the cells from shear-induced damage and facilitates cancer cell colonization (63). In addition, these collagens and collagenases are also involved in multiple tumor-associated pathways, such as the PI3K-Akt and tyrosine kinase receptor signaling pathways. Therefore, matrix collagens and their associated collagenases can affect the development and progression of CRC in multiple ways.

The present study provides multi-level evidence for the importance of abnormal collagen remodeling in the development and prognostic evaluation of CRC from the aspects of collagen arrangement, related proteins and their coding genes. Dense matrix collagen at the tumor invasion front can promote tumor invasion, which provides a novel pathological direction of analysis for clinicians. Because different types of collagen and collagenases interact with each other in the matrix, combination analysis of multiple biomarkers may improve the reliability of clinical evaluation, suggesting that the evaluation of matrix collagen in CRC should not focus on only a single type collagen. Finally, matrix collagens and collagenases can influence the development of CRC by activating platelets and other tumor-associated pathways, which may provide the reference direction for subsequent treatment.

The main limitation of the present study is the relatively small sample size. Larger-scale functional studies are required to improve our understanding of the effects of matrix collagens and their associated collagenases in CRC. However, the results provide some interesting suggestions for future studies with an increased sample size.

Availability of data and materials

The STRING, Oncomine, TCGA, GEO and PROGgeneV2 material is publicly available. The datasets used and analyzed during the current study are available from the corresponding author on reasonable request.

Authors' contributions

YL conceived and designed the experiments. YL and ZL performed the experiments and analyzed the data. GH, HL and JQ contributed to the acquisition of the data. YL, ZL and FN have made substantial contribution to the collection of tissue samples. YL and GH wrote the manuscript. BW, as the corresponding author, was responsible for project funding, design, writing and checking. All authors have examined the manuscript. All authors read and approved the manuscript and agree to be accountable for all aspects of the research in ensuring that the accuracy or integrity of any part of the work are appropriately investigated and resolved.

Ethics approval and consent to participate

The experiment was approved by the First Affiliated Hospital of Guangzhou University of Chinese Medicine. This study was approved by the Ethics Committee of the First Affiliated Hospital of Guangzhou University of Chinese Medicine [No. Y (2019)172] and informed consent was obtained from all patients. This study was performed in accordance with the Declaration of Helsinki.

Patient consent for publication

Not applicable.

Competing interests

The authors have declared that no competing interest exists.

References

1. Bray F, Ferlay J, Soerjomataram I, Siegel RL, Torre LA and Jemal A: Global cancer statistics 2018: GLOBOCAN estimates of incidence and mortality worldwide for 36 cancers in 185 countries. CA Cancer J Clin 68: 394-424, 2018.
2. Turajlic S and Swanton C: Metastasis as an evolutionary process. Science 352: 169-175, 2016.
3. Crotti S, Piccoli M, Rizzolio F, Giordano A, Nitti D and Agostini M: Extracellular matrix and colorectal cancer: How surrounding microenvironment affects cancer cell behavior? J Cell Physiol 232: 967-975, 2017.
4. Provenzano PP, Eliceiri KW, Campbell JM, Inman DR, White JG and Keely PJ: Collagen reorganization at the tumor-stromal interface facilitates local invasion. BMC Med 4: 38, 2006.
5. Chen D, Chen G, Jiang W, Fu M, Liu W, Sui J, Xu S, Liu Z, Zheng X, Chi L, *et al*: Association of the collagen signature in the tumor microenvironment with lymph node metastasis in early gastric cancer. JAMA Surg 154: e185249, 2019.
6. Huynh RN, Yousof M, Ly KL, Gombedza FC, Luo X, Bandyopadhyay BC and Raub CB: Microstructural densification and alignment by aspiration-ejection influence cancer cell interactions with three-dimensional collagen networks. Biotechnol Bioeng 117: 1826-1838, 2020.
7. Conklin MW and Keely PJ: Why the stroma matters in breast cancer: Insights into breast cancer patient outcomes through the examination of stromal biomarkers. Cell Adh Migr 6: 249-260, 2012.
8. Whatcott CJ, Diep CH, Jiang P, Watanabe A, LoBello J, Sima C, Hostetter G, Shepard HM, Von Hoff DD and Han H: Desmoplasia in primary tumors and metastatic lesions of pancreatic cancer. Clin Cancer Res 21: 3561-3568, 2015.
9. Bonnans C, Chou J and Werb Z: Remodelling the extracellular matrix in development and disease. Nat Rev Mol Cell Biol 15: 786-801, 2014.
10. Beam J, Botta A, Ye J, Soliman H, Matier BJ, Forrest M, MacLeod KM and Ghosh S: Excess linoleic acid increases collagen I/III ratio and 'stiffens' the heart muscle following high fat diets. J Biol Chem 290: 23371-23384, 2015.
11. Najafi M, Farhood B and Mortezaee K: Extracellular matrix (ECM) stiffness and degradation as cancer drivers. J Cell Biochem 120: 2782-2790, 2019.
12. Brauchle E, Kasper J, Daum R, Schierbaum N, Falch C, Kirschniak A, Schäffer TE and Schenke-Layland K: Biomechanical and biomolecular characterization of extracellular matrix structures in human colon carcinomas. Matrix Biol 68-69: 180-193, 2018.
13. Paul CD, Hruska A, Staunton JR, Burr HA, Daly KM, Kim J, Jiang N and Tanner K: Probing cellular response to topography in three dimensions. Biomaterials 197: 101-118, 2019.
14. Tanjore H and Kalluri R: The role of type IV collagen and basement membranes in cancer progression and metastasis. Am J Pathol 168: 715-717, 2006.
15. Hua H, Li M, Luo T, Yin Y and Jiang Y: Matrix metalloproteinases in tumorigenesis: An evolving paradigm. Cell Mol Life Sci 68: 3853-3868, 2011.
16. Tjin G, White ES, Faiz A, Sicard D, Tschumperlin DJ, Mahar A, Kable EPW and Burgess JK: Lysyl oxidases regulate fibrillar collagen remodelling in idiopathic pulmonary fibrosis. Dis Model Mech 10: 1301-1312, 2017.
17. Wong CC, Tse AP, Huang YP, Zhu YT, Chiu DK, Lai RK, Au SL, Kai AK, Lee JM, Wei LL, *et al*: Lysyl oxidase-like 2 is critical to tumor microenvironment and metastatic niche formation in hepatocellular carcinoma. Hepatology 60: 1645-1658, 2014.
18. Shiozawa J, Ito M, Nakayama T, Nakashima M, Kohno S and Sekine I: Expression of matrix metalloproteinase-1 in human colorectal carcinoma. Mod Pathol 13: 925-933, 2000.
19. Moreno-Bueno G, Salvador F, Martín A, Floristán A, Cuevas EP, Santos V, Montes A, Morales S, Castilla MA, Rojo-Sebastián A, *et al*: Lysyl oxidase-like 2 (LOXL2), a new regulator of cell polarity required for metastatic dissemination of basal-like breast carcinomas. EMBO Mol Med 3: 528-544, 2011.
20. Liu Y, Zhang J, Chen Y, Sohel H, Ke X, Chen J and Li YX: The correlation and role analysis of COL4A1 and COL4A2 in hepatocarcinogenesis. Aging (Albany NY) 12: 204-223, 2020.
21. Zhao S and Yu M: Identification of MMP1 as a potential prognostic biomarker and correlating with immune infiltrates in cervical squamous cell carcinoma. DNA Cell Biol 39: 255-272, 2020.
22. Sugai T, Yamada N, Eizuka M, Sugimoto R, Uesugi N, Osakabe M, Ishida K, Otsuka K, Sasaki A and Matsumoto T: Vascular invasion and stromal S100A4 expression at the invasive front of colorectal cancer are novel determinants and tumor prognostic markers. J Cancer 8: 1552-1561, 2017.
23. Xiaopei H, Kunfu D, Lianyuan T, Zhen L, Mei X and Haibo Y: Tumor invasion front morphology: A novel prognostic factor for intrahepatic cholangiocarcinoma. Eur Rev Med Pharmacol Sci 23: 9821-9828, 2019.
24. Brierley J, Gospodarowicz M and Wittekind C: International Union Against Cancer: TNM Classification of Malignant Tumours. 8th edition. Wiley-Blackwell, West Sussex, United Kingdom, 2017.
25. Coelho PGB, Souza MV, Conceição LG, Viloria MIV and Bedoya SAO: Evaluation of dermal collagen stained with picrosirius red and examined under polarized light microscopy. An Bras Dermatol 93: 415-418, 2018.
26. Szklarczyk D, Gable AL, Lyon D, Junge A, Wyder S, Huerta-Cepas J, Simonovic M, Doncheva NT, Morris JH, Bork P, *et al*: STRING v11: Protein-protein association networks with increased coverage, supporting functional discovery in genome-wide experimental datasets. Nucleic Acids Res 47: D607-D613, 2019.
27. Cline MS, Craft B, Swatloski T, Goldman M, Ma S, Haussler D and Zhu J: Exploring TCGA Pan-Cancer data at the UCSC cancer genomics browser. Sci Rep 3: 2652, 2013.
28. Huang da W, Sherman BT and Lempicki RA: Systematic and integrative analysis of large gene lists using DAVID bioinformatics resources. Nat Protoc 4: 44-57, 2009.
29. Smith JJ, Deane NG, Wu F, Merchant NB, Zhang B, Jiang A, Lu P, Johnson JC, Schmidt C, Bailey CE, *et al*: Experimentally derived metastasis gene expression profile predicts recurrence and death in patients with colon cancer. Gastroenterology 138: 958-968, 2010.
30. Mizukami A, Matsue Y, Naruse Y, Kowase S, Kurosaki K, Suzuki M, Matsumura A, Nogami A, Aonuma K and Hashimoto Y: Kaplan-Meier survival analysis and Cox regression analyses regarding right ventricular septal pacing: Data from Japanese pacemaker cohort. Data Brief 8: 1303-1307, 2016.
31. Goswami CP and Nakshatri H: PROGgeneV2: Enhancements on the existing database. BMC Cancer 14: 970, 2014.
32. Marisa L, de Reyniès A, Duval A, Selves J, Gaub MP, Vescovo L, Etienne-Grimaldi MC, Schiappa R, Guenot D, Ayadi M, *et al*: Gene expression classification of colon cancer into molecular subtypes: Characterization, validation, and prognostic value. PLoS Med 10: e1001453, 2013.
33. Ritchie ME, Phipson B, Wu D, Hu Y, Law CW, Shi W and Smyth GK: Limma powers differential expression analyses for RNA-sequencing and microarray studies. Nucleic Acids Res 43: e47, 2015.
34. Junqueira LC, Cossermelli W and Brentani R: Differential staining of collagens type I, II and III by Sirius Red and polarization microscopy. Arch Histol Jpn 41: 267-274, 1978.
35. Kalluri R: Basement membranes: Structure, assembly and role in tumour angiogenesis. Nat Rev Cancer 3: 422-433, 2003.

36. Deryugina EI and Quigley JP: Matrix metalloproteinases and tumor metastasis. Cancer Metastasis Rev 25: 9-34, 2006.
37. Hsu TI, Lin SC, Lu PS, Chang WC, Hung CY, Yeh YM, Su WC, Liao PC and Hung JJ: MMP7-mediated cleavage of nucleolin at Asp255 induces MMP9 expression to promote tumor malignancy. Oncogene 36: 875-876, 2017.
38. Zhou D, Tian Y, Sun L, Zhou L, Xiao L, Tan RJ, Tian J, Fu H, Hou FF and Liu Y: Matrix metalloproteinase-7 is a urinary biomarker and pathogenic mediator of kidney fibrosis. J Am Soc Nephrol 28: 598-611, 2017.
39. Imai K, Yokohama Y, Nakanishi I, Ohuchi E, Fujii Y, Nakai N and Okada Y: Matrix metalloproteinase 7 (matrilysin) from human rectal carcinoma cells activation of the precursor, interaction with other matrix metalloproteinases and enzymic properties. J Biol Chem 270: 6691-6697, 1995.
40. Kim YM, Kim EC and Kim Y: The human lysyl oxidase-like 2 protein functions as an amine oxidase toward collagen and elastin. Mol Biol Rep 38: 145-149, 2011.
41. López-Jiménez AJ, Basak T and Vanacore RM: Proteolytic processing of lysyl oxidase-like-2 in the extracellular matrix is required for crosslinking of basement membrane collagen IV. J Biol Chem 292: 16970-16982, 2017.
42. Chiang WF, Liu SY, Fang LY, Lin CN, Wu MH, Chen YC, Chen YL and Jin YT: Overexpression of galectin-1 at the tumor invasion front is associated with poor prognosis in early-stage oral squamous cell carcinoma. Oral Oncol 44: 325-334, 2008.
43. Zhou ZH, Ji CD, Xiao HL, Zhao HB, Cui YH and Bian XW: Reorganized collagen in the tumor microenvironment of gastric cancer and its association with prognosis. J Cancer 8: 1466-1476, 2017.
44. Pang MF, Siedlik MJ, Han S, Stallings-Mann M, Radisky DC and Nelson CM: Tissue stiffness and hypoxia modulate the integrin-linked kinase ILK to control breast cancer stem-like cells. Cancer Res 76: 5277-5287, 2016.
45. Cackowski FC, Wang Y, Decker JT, Sifuentes C, Weindorf S, Jung Y, Wang Y, Decker AM, Yumoto K, Szerlip N, et al: Detection and isolation of disseminated tumor cells in bone marrow of patients with clinically localized prostate cancer. Prostate 79: 1715-1727, 2019.
46. Ray A, Slama ZM, Morford RK, Madden SA and Provenzano PP: Enhanced directional migration of cancer stem cells in 3D aligned collagen matrices. Biophys J 112: 1023-1036, 2017.
47. Tilbury K, Lien CH, Chen SJ and Campagnola PJ: Differentiation of Col I and Col III isoforms in stromal models of ovarian cancer by analysis of second harmonic generation polarization and emission directionality. Biophys J 106: 354-365, 2014.
48. Fan HX, Li HX, Chen D, Gao ZX and Zheng JH: Changes in the expression of MMP2, MMP9, and ColIV in stromal cells in oral squamous tongue cell carcinoma: Relationships and prognostic implications. J Exp Clin Cancer Res 31: 90, 2012.
49. Öhlund D, Franklin O, Lundberg E, Lundin C and Sund M: Type IV collagen stimulates pancreatic cancer cell proliferation, migration, and inhibits apoptosis through an autocrine loop. BMC Cancer 13: 154, 2013.
50. Wang J, Boddupalli A, Koelbl J, Nam DH, Ge X, Bratlie KM and Schneider IC: Degradation and remodeling of epitaxially grown collagen fibrils. Cell Mol Bioeng 12: 69-84, 2019.
51. Barker HE, Chang J, Cox TR, Lang G, Bird D, Nicolau M, Evans HR, Gartland A and Erler JT: LOXL2-mediated matrix remodeling in metastasis and mammary gland involution. Cancer Res 71: 1561-1572, 2011.
52. Zhou CX, Gao Y, Johnson NW and Gao J: Immunoexpression of matrix metalloproteinase-2 and matrix metalloproteinase-9 in the metastasis of squamous cell carcinoma of the human tongue. Aust Dent J 55: 385-389, 2010.
53. Liu M, Hu Y, Zhang MF, Luo KJ, Xie XY, Wen J, Fu JH and Yang H: MMP1 promotes tumor growth and metastasis in esophageal squamous cell carcinoma. Cancer Lett 377: 97-104, 2016.
54. Ma HP, Chang HL, Bamodu OA, Yadav VK, Huang TY, Wu ATH, Yeh CT, Tsai SH and Lee WH: Collagen 1A1 (COL1A1) is a reliable biomarker and putative therapeutic target for hepatocellular carcinogenesis and metastasis. Cancers (Basel) 11: 786, 2019.
55. Misawa K, Mochizuki D, Imai A, Mima M, Misawa Y and Mineta H: Analysis of site-specific methylation of tumor-related genes in head and neck cancer: Potential utility as biomarkers for prognosis. Cancers (Basel) 10: 27, 2018.
56. Su B, Zhao W, Shi B, Zhang Z, Yu X, Xie F, Guo Z, Zhang X, Liu J, Shen Q, et al: Let-7d suppresses growth, metastasis, and tumor macrophage infiltration in renal cell carcinoma by targeting COL3A1 and CCL7. Mol Cancer 13: 206, 2014.
57. Wang T, Hou J, Jian S, Luo Q, Wei J, Li Z, Wang X, Bai P, Duan B, Xing J and Cai J: miR-29b negatively regulates MMP2 to impact gastric cancer development by suppress gastric cancer cell migration and tumor growth. J Cancer 9: 3776-3786, 2018.
58. Nabais Sá MJ, Storey H, Flinter F, Nagel M, Sampaio S, Castro R, Araújo JA, Gaspar MA, Soares C, Oliveira A, et al: Collagen type IV-related nephropathies in Portugal: Pathogenic COL4A3 and COL4A4 mutations and clinical characterization of 25 families. Clin Genet 88: 456-461, 2015.
59. Takeuchi M, Yamaguchi S, Yonemura S, Kakiguchi K, Sato Y, Higashiyama T, Shimizu T and Hibi M: Type IV collagen controls the axogenesis of cerebellar granule cells by regulating basement membrane integrity in Zebrafish. PLoS Genet 11: e1005587, 2015.
60. Mammadova-Bach E, Zigrino P, Brucker C, Bourdon C, Freund M, De Arcangelis A, Abrams SI, Orend G, Gachet C and Mangin PH: Platelet integrin α6β1 controls lung metastasis through direct binding to cancer cell-derived ADAM9. JCI Insight 1: e88245, 2016.
61. Lavergne M, Janus-Bell E, Schaff M, Gachet C and Mangin PH: Platelet integrins in tumor metastasis: Do they represent a therapeutic target? Cancers (Basel) 9: 133, 2017.
62. Repsold L, Pool R, Karodia M, Tintinger G and Joubert AM: An overview of the role of platelets in angiogenesis, apoptosis and autophagy in chronic myeloid leukaemia. Cancer Cell Int 17: 89, 2017.
63. Egan K, Cooke N and Kenny D: Living in shear: Platelets protect cancer cells from shear induced damage. Clin Exp Metastasis 31: 697-704, 2014.